Title	Reduced graphene oxide for the development of wearable mechanical energy-harvesters: A review
Authors	Nag, Anindya;Simorangkir, Roy B. V. B.;Sapra, Samta;Buckley, John L.;O'Flynn, Brendan;Liu, Zhi;Mukhopadhyay, Subhas Chandra
Publication date	2021-10-06
Original Citation	Nag, A., Simorangkir, R. B. V. B., Sapra, S., Buckley, J. L., O'Flynn, B., Liu, Z. and Mukhopadhyay, S. C. (2021) 'Reduced graphene oxide for the development of wearable mechanical energy-harvesters: A review', IEEE Sensors Journal. doi: 10.1109/JSEN.2021.3118565
Type of publication	Article (peer-reviewed)
Link to publisher's version	10.1109/JSEN.2021.3118565
Rights	© 2021, IEEE. Personal use of this material is permitted. Permission from IEEE must be obtained for all other uses, in any current or future media, including reprinting/republishing this material for advertising or promotional purposes, creating new collective works, for resale or redistribution to servers or lists, or reuse of any copyrighted component of this work in other works.
Download date	2023-05-05 05:39:48
Item downloaded from	http://hdl.handle.net/10468/12079

Reduced graphene oxide for the development of wearable mechanical energy-harvesters: A review

Anindya Nag, *Member, IEEE,* Roy B. V. B. Simorangkir, *Member, IEEE*, Samta Sapra, *Student Member, IEEE*, John L. Buckley, *Member, IEEE*, Brendan O'Flynn, *Senior Member, IEEE*, Zhi Liu, and Subhas Chandra Mukhopadhyay, *Fellow, IEEE*

***Abstract*—The unique characteristics of graphene have generated a lot of interest in the research community. A concept of utilizing graphene and its derivatives in the development of energy harvesters has just appeared in recent decades. This paper focuses on the application of reduced graphene oxide (rGO), a graphene derivative, in the development of wearable mechanical energy-harvesters to enable self-powered wearable sensing systems. Harvesting of energy has been a state-of-the-art phenomenon due to the ever-increasing requirement of power to run the sensing systems. Flexible systems that used rGO to gather energy with intensities ranging from a few microwatts to a few hundreds of microwatts have been used. Some examples are presented, focusing on the class of piezoelectric and triboelectric-based energy harvesters, with descriptions of their material composition, manufacturing methods, operating principle, and performance. Finally, the challenges and drawbacks of rGO-based energy harvesters are discussed, along with some of the potential solutions.**

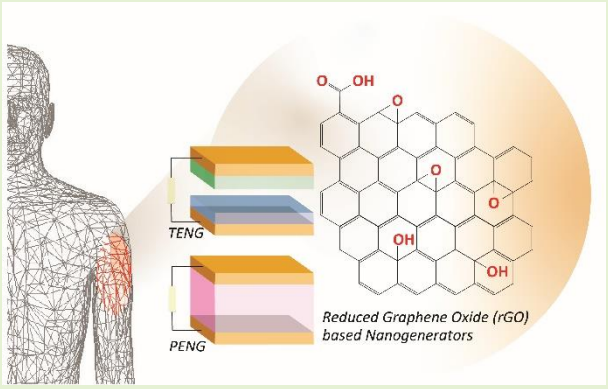

***Index Terms*—Graphene, mechanical energy-harvesting, piezoelectric, reduced graphene oxide, triboelectric**

I. Introduction

The concept of energy scavenging devices has received significant growth in the past decades, especially due to the ever-growing desire to generate portable and wireless wearable electronics with prolonged lifespans [1-7]. In the case of portable electronics, electrochemical batteries, e.g., lithium-ion batteries, have been used as the main solution of power source, which unfortunately has limited lifespans. This can be cumbersome, especially when the system is to be placed at a remote location or performs specific functions that require a continuous source of energy. Also, lithium-ion batteries are often bulky, rigid, and susceptible to an explosion, thus may not be suitable for the emerging wearable applications, which impose extra requirements of users' convenience and safety. Some advancements have been made in the development of flexible and stretchable batteries [8, 9]. However, they still need to be charged or even replaced periodically, which can burden not only the users but also the environment. This has therefore motivated the development of devices that can harvest the surrounding energy and convert it into electrical energy.

In the context of wearable electronics, the human body as the operating environment has a variety of energy sources, including thermal, chemical, and mechanical forms, among which mechanical form being the most abundant [10]. Fig. 1 depicts one such concept of a self-powered wearable smart system, where the movement of an individual is converted into electrical energy via coupling of inductive and triboelectric effects to power a multiplexed sweat sensing [11]. The human motion energy harvesting device is embedded with microfluidic-based sweat biosensing, signal processing unit, and Bluetooth-based wireless module for real-time transmission to the mobile user interface.

In the process of converting mechanical to electrical energy, state-of-the-art mechanical energy harvesters generally involves electromagnetic [12, 13], electrostatic [14, 15], piezoelectric [16, 17], and triboelectric mechanisms [18-20]. The last two methods have grown in popularity in recent decades due to their advantages, which include greater output voltage and power density, relatively low-cost and simple design, fabrication, and implementation, particularly in the context of wearable electronics [21, 22]. Unlike the

This work was supported in part by the Enterprise Ireland funded HOLISTICS DTIF project (EIDT20180291-A), as well as by Science Foundation Ireland (SFI) under the following Grant Numbers: Connect Centre for Future Networks and Communications (13/RC/2077) and the Insight Centre for Data Analytics (SFI/12/RC/2289), as well as the European Regional Development Fund.

Anindya Nag and Zhi Liu are with the School of Information Science and Engineering, Shandong University, Jinan, China (Email: anindya1991@gmail.com, liuzhi@sdu.edu.cn).

Roy B. V. B. Simorangkir, John L. Buckley, and Brendan O'Flynn are with the Tyndall National Institute, University College Cork, Dyke Parade, T12R5CP Cork, Ireland

Samta Sapra and Subhas Chandra Mukhopadhyay are with the Faculty of Science and Engineering, Macquarie University, Sydney, NSW 2109, Australia.

electromagnetic and electrostatic-based energy harvesting approaches, piezoelectric and triboelectric-based techniques may function across a large frequency range, which is useful given that mechanical vibration is often highly variable. After the first presentation of nanogenerator ideas in 2006 [23], which opened up new horizons for self-powered wearable electronics, the popularity of piezoelectric and triboelectric based energy harvesters rose even more. Since then, research into the development of nanomaterials and structures for effective mechanical to electrical energy conversion through piezoelectric and triboelectric phenomena has gained a great deal of traction. Nanogenerators with mechanical flexibility feature have also been developed more recently [24-26] and they show a lot of promise in terms of offering energy production options for compliant and stretchable electronics. In light of the foregoing, this paper will concentrate on the class of piezoelectric nanogenerator (PENG) and triboelectric nanogenerator (TENG) energy harvesters.

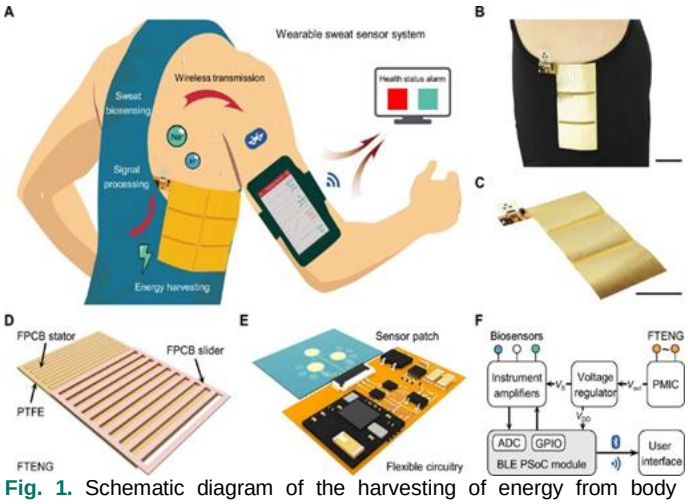

Fig. 1. Schematic diagram of the harvesting of energy from body motions and simultaneously send the data through wireless transmitting unit. The sensing system also consisted of a conditioning circuit that processed the sensed data prior to sending them to the monitoring unit [11].

For the creation PENG and TENG energy harvesters, many possibilities for material selection have been reported. Some examples of piezoelectic materials include wurtzite zinc oxide (ZNO) thin films [27], perovskite lead zirconate titanate (PZT) nanofibers [28], polyvinylidenefluoride (PVDF) polymer [29], Indium Nitride (InN) [30], Galium Nitride (GaN) nanowires [31], Cadnium Sulfide (CdS) nanowires [32], to name a few. On the other hand, nearly all materials exhibit a triboelectric effect, allowing for a wide range of options. Polytetrafluoroethylene (PTFE), Kapton, polydimethylsiloxane (PDMS), polyester, fluorinated ethylene propylene (FEP), polystyrene (PS), silicone, wool, nylon, and acrylics, are some of the most common triboelectric materials used [10, 33].

A novel notion for using graphene in the development of energy harvester has recently emerged. Graphene has sparked a lot of attention in the research community since its initial appearance in 2004 [34] as a result of micromechanical cleavage separation from graphite. In the context of energy harvesting systems, graphene has been hailed as a promising material for its energy transduction capability, which is backed up by several other notable characteristics [35, 36]. Graphene is unique in that it has a high transmission capacity with a single heterogeneous transfer of electrons and charge rate, as well as a high electrocatalytic properties. The structure of graphene is also resilient, thanks to a two-dimensional layer of carbon atoms with sp^2 hybridization that are connected in a rigid hexagonal lattice, Furthermore, graphene sheets may also be arranged into three-dimensional porous structures with a large specific surface area, abundant nanopores, hierarchically linked networks and channels, great electrochemical stability, high electrical conductivity, and exceptional mechanical flexibility. All of the aforementioned qualities contribute to the efficient electric energy generation process.

In this article, we present a comprehensive review on the utilization of reduced graphene oxide (rGO), a kind of graphene derivative, to realize piezoelectric and triboelectric-based energy harvesters. Despite the numerous reviews on graphene, its derivatives and their wide range of applications [35-47], as well as on different mechanical energy harvesters and associated technologies [10, 14, 17, 18, 22, 33, 48-55], there has yet to be a review on the implementation of the emerging rGO for mechanical energy harvesting. The remainder of the paper is laid out as follows. We began by presenting a general context for rGO as a graphene derivative, followed by an overview of the various mechanical energy harvesters and their operating principles. Following that, we present a few noteworthy instances of rGO-based piezoelectric and triboelectric energy harvesters and provide details on their material compositions, manufacturing approaches, and performance. Some challenges with the existing technologies have also been discussed, along with some possible remedies. The future opportunities in terms of commercial and academic uses have also been showcased in this paper.

II. Pristine Graphene, Graphene Oxide (GO) and Reduced Graphene Oxide (rGO)

Graphene is a honeycomb-shaped atomically thin two-dimensional (2D) sheet of sp^2 carbon atoms. Despite the exceptional characteristics mentioned in the preceding section, pristine graphene implementation has proven problematic due to difficult bottom-up synthesis [36], low solubility [56], and agglomeration in solution due to van der Waals surface interactions [37]. As a result, several research efforts have been made to synthesize compounds having structures comparable to pristine graphene, known as graphene derivatives [36, 39, 44, 45]. The objective is to achieve as many of the benefits of pristine graphene as feasible. Among them, graphene oxide (GO) and rGO have received a lot of interest including in the development of energy harvesting devices.

GO is a chemically modified graphene with oxygen functional groups such as epoxides, alcohols, and carboxylic acids on the basal plane [57-59]. According to chemical analysis, the carbon to oxygen ratio of GO is around three to one [60]. GO can be produced from graphite oxide through sonication, stirring, or combination of these methods [61]. Graphite oxide can be synthesized through oxidation of graphite in protonated solvents [61]. GO has the particular benefit of being well-dispersed in aqueous polar solvents like water [39, 62, 63], allowing for simple scalable mass production [64], however it may not be compatible with most

of organic polymer nanocomposites [37]. Because of the large number of oxygen functional groups in GO, unlike pristine graphene, GO is electrically insulating [37, 65], making it unsuitable for the synthesis of conducting nanocomposites.

Chemical techniques utilizing reductants such as hydrazine [60, 66], dimethylhydrazine [67], hydroquinon [68], and $NaBH_4$ [69], thermal method [70, 71], and ultraviolet-assisted method [72], can restore conductivity of GO by several orders of magnitude, resulting in what is known as rGO. The thermal reduction method, which is generally accomplished by high-temperature vacuum annealing, usually yields a considerably more effective reduction, restoring sp^2 carbon domains and enhancing GO's electrical and thermal properties [73, 74]. Although none of these techniques remove the oxygen groups completely, they do allow for the production of graphene derivative, rGO, that is more similar to pristine graphene than GO. The incorporation of rGO in PENG and TENG energy harvesters, in particular, gives numerous performance benefits. The use of rGO as nanofillers in PENG enhances the formation of dipoles which act as micro-capacitors in the composites, resulting in improved charge generation and storage in the resultant electrodes [75]. It also aids the enhancement of β-phase crystallization as well as crystallinity of particular classes of piezoelectric polymers, therefore enhancing the piezoelectric nature of the end products [76-78]. In the case of TENG, the presence of oxygen functional groups and defects improves the electrodes' tribo-negative contact, which is advantageous during triboelectrification and electrostatic induction processes [49, 79]. The nonvolatile electron-trapping characteristic of rGO [58, 80] further increases surface charge density of triboelectric materials [81].

III. Mechanical Energy Harvesting Mechanisms

Mechanical energy, widely existing in an ambient environment with a variety of forms and wide-range of scales, recently becomes an attractive target for energy harvesting. In this section, the fundamentals of different mechanisms that can be employed to convert mechanical to electrical energy are briefly discussed.

A. Electromagnetic Generators

The mechanical to electrical energy conversion in this class of generator is based on the concept of electromagnetic induction discovered by Faraday in 1831. The generator principally involves a conductor, typically in the form of coil, and permanent magnet. The electricity is generated by either the relative movement of the magnet and the coil, or due to the changes in the magnetic field. The amount of electricity produced is typically a function of the magnetic field strength, the relative movement velocity and the coil's number of turns. One effective implementation can be seen in Fig. 2 developed by El-hami et al for a macro electromagnetic generator [82]. The generator consists of a cantilever beam with two NdFeB magnets mounted on a C-shape core at the free end of the beam. Between the poles of the magnets, the coil made up of many turns of enamelled copper wire was added. Upon periodic vibration of the beam which was made possible due to the magnets also acting as inertial masses, the relative displacement of the magnet drives the generation of the electrical energy. A power output in excess of 1mW was reported at a vibration frequency of 320 Hz.

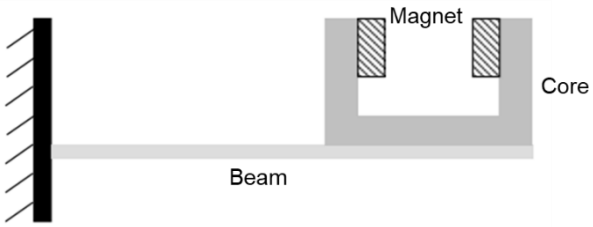

Fig. 2. Macro electromagnetic generator by El-hami et al [82].

B. Electrostatic Generators

This sort of generator generates electrical energy primarily through the use of a MEMS variable capacitor, which works by depositing charge on the capacitor plates and then moving them apart. When a battery of voltage charges the plates, it forms equal but opposite charges on the plates, resulting in charge storage when the voltage source is disconnected. When the plates are separated, an electrostatic field is built which drives the electrons to flow through the external circuit. The electrostatic generator developed by Meninger et al [14] is shown in Fig. 3 as an implementation example . The interdigitated combs move together and apart following the oscillation of the mass, which thus changes the area of the variable capacitor and hence its capacitance. The change in capacitance of the interdigitated combs as viewed from their electric terminals governs the passage of energy from the spring-mass system to the electrical circuit. The change of capacitance must be maximized to optimize this energy transfer by considering the given limits of space and structural soundness.

Electrostatic generator can be categorized into three: (1) in-plane overlap varying, (2) in-plane gap closing, and (3) out-of-plane gap closing [83]. This type of generator can also be operated in either charge constrained or voltage constrained.

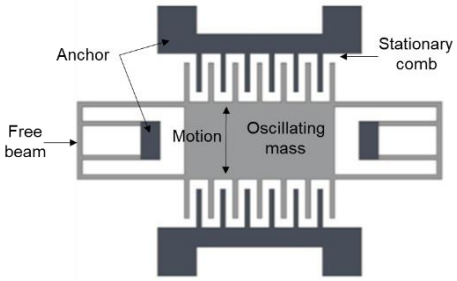

Fig. 3. Electrostatic generator by Meninger et al [14].

C. Piezoelectric Generators

In this type of generator, the mechanical to electrical energy conversion takes advantage of the particular properties of piezoelectric material attached to the electrodes. The mutual displacement of anions and cations in the crystal produces an electric dipole moment in this material, as shown in Fig. 4, when exposed to mechanical strain [7]. As a result, there is an internal piezoelectric potential difference in the direction of

external force, resulting in a continuous alternate pulse current being generated in the external circuit.

Piezoelectric materials are available in many forms including single crystal (e.g., quartz), thin film (e.g., sputtered zinc oxide), piezoceramic (e.g., lead zirconate titanate or PZT), and polymeric materials such as polyvinylidenefluoride (PVDF). Piezoelectric materials are also anisotropic, meaning that the level of piezoelectricity obtained varies depending upon the direction of the applied forces and the orientation of the electrodes [48].

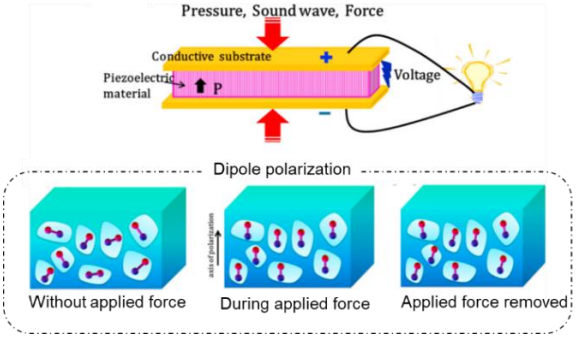

Fig. 4. Working principle of piezoelectric generator [7].

D. Triboelectric Generators

The mechanical to electrical energy conversion of this type of generator relies on the coupling effects of triboelectrification and electrostatic induction. Triboelectrification is a generation of electrostatic charges on the surface of two different materials upon contact. The generated triboelectric charges on the two surfaces are same in number but different in polarity. Therefore, when the two layers are separated, an electrostatic field is built. Periodic motion of contacting-separating or sliding between the two dielectric surfaces creates a periodic potential differences between two electrodes attached to the dielectric which results in an alternating current output flow through the external circuit. Some physical parameters such as the microstructures and surface patterns, particle size and load stress are pivotal and needs to be optimized as they determine the attributes of charge injection depth, surface charge density and movement of electrons, which are crucial in the energy conversion process. Four fundamental working modes of triboelectric generator is given in Fig. 5, which include vertical contact-separation mode, lateral sliding mode, single-electrode mode, and freestanding mode [51, 52, 84, 85]. Among these modes, most of triboelectric generators function with vertical contact-separation mode.

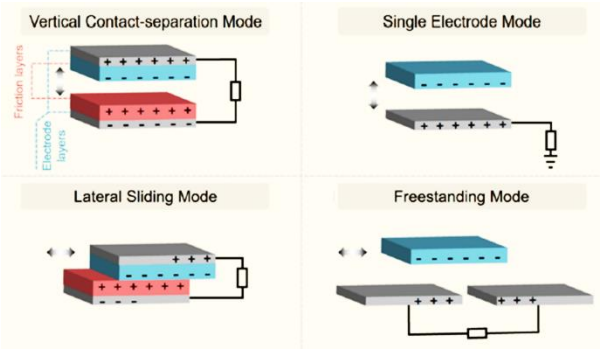

Fig. 5. Fundamental mechanism of triboelectric generator [52].

IV. rGO BASED PENG AND TENG ENERGY-HARVESTERS

There has been a growing effort in the exploration of rGO for development of efficient mechanical energy harvesters. This section showcases some advancements in the piezoelectric and triboelectric-based energy harvesters recently reported, particularly those that involve rGO with other metals and polymers at optimized proportions.

A. Examples of PENG energy-harvesters

The work in [24] demonstrated the development of a flexible self-poled PENG using PVDF, rGO and silver nanoparticles (Ag NPs) composite. Fig. 6 shows the schematic diagram of the associated fabrication process. GO synthesized using the modified Hummers' method was reduced and mixed with metallic nanoparticles and piezoelectric polymers using magnetic stirring, ultrasonication and curing processes. Then, aluminum foils were attached to the nanocomposite films, followed by connecting copper films between the nanocomposite and aluminum foils. Finally, the prototypes were encapsulated using PDMS films to provide a protection from water and dust. The β and γ piezoelectric phases of PVDF were enhanced by the presence of dual nanomaterials, rGO and Ag NPs. The sensors displayed an energy density of 0.26 J/cm in the presence of an external field of 148 kV/cm. The pressure applied by fixing human fingers was enough to light up twenty commercial blue light-emitting diodes (LEDs). The peak open-circuit voltage (V_{oc}), short-circuit current (I_{sc}), peak power density obtained by these sensors were 18 V, 1.05 μA and 28 W/m^3, respectively. The efficiency of the developed device was around 0.65%.

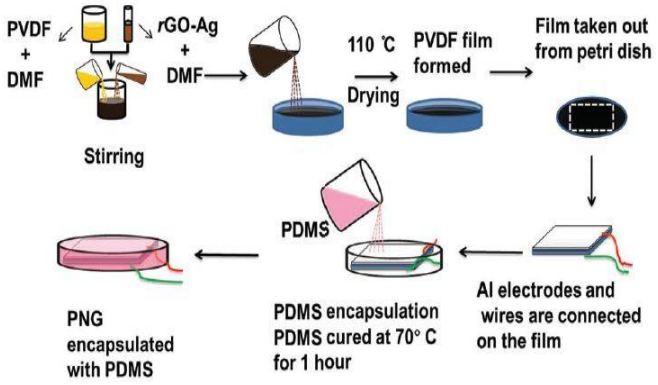

Fig. 6. Schematic diagram of the fabrication process of rGO/Ag NPs/PVDF-based PENG [24].

Another example showing the use of rGO for developing PENG-based energy-harvesters can be seen in [86], where the nanocomposites were formed using poly(vinylidene fluoride-trifluoroethylene) (PVDF-TrFE) and barium titanate ($BaTiO_3$). The synthesis process was carried out by spin-coating five different composites over copper(Cu)/Polyethylene Terephthalate (PET) substrates. Four out of five composites included rGO at different values and one did not. These samples were then annealed, while the electrodes were attached with platinum (Pt) wires using silver epoxy. This was followed by another spin-coating process where a thin-film layer of PDMS was formed on top of PDMS as a packaging layer. The last step included the exertion of poling process to align the ferroelectric

dipoles of the PVDF-TrFE and BTO. The surface area of these devices was 3 cm x 2.5 cm. The fabrication of the sensors was carried out by opting for an optimized value of rGO of 0.5 wt.% to obtain a maximum output performance. When a force of 2N was applied, the highest voltage and current acquired by these PENG devices were 8.5 V and 2 μA, respectively. Other attributes of the sensors included high stability and reproducibility of the results.

An interesting work showing the use of rGO-based composites for energy-harvesting applications can be seen in the research done by Bhunia et al. [25]. This work explains the dual effects of TENG and PENG for harvesting power in the milliwatt range. The sensors were formed using nanocomposites developed by mixing sol-gel processed rGO and PVDF-TrFE to induce effects of PENG and hybridized piezoelectric TENG (HPTENG). The resultant nanocomposites having strong interaction between rGO and PVDF-TrFE broke the centrosymmetric of rGO, thus obtaining piezoelectric, ferroelectric and triboelectric properties. Graphite powder was treated through the modified Hummers' method followed by oxidization to form GO, which was subsequently used to form dispersions by mixing DI water. The resultant samples were then reduced to form rGO by reacting with hydrazine hydrate and heating at 100˚C for 24 hours. After preparing by mixing different weight ratios of rGO and PVDF-TrFE, each solution was spin-coated on ITO-coated glass substrates. The final steps included the exertion of annealing and rapid ice quenching processes on the samples. The PENG and HPTENG devices were able to obtain the highest voltages of 89.7 V and 227 V, respectively, for an optimized value (0.5 wt.%) of rGO mixed in the composites. The maximum output power densities for the PENG and HPTENG prototypes were 0.28 W/cm^3 and 0.34 W/cm^3, respectively.

The use of in situ polarization technique on PVDF-TrFE films to improve the β-phase prior to mixing them with rGO can be seen in the work done by Hu et al. [75]. The poling of PVDF-TrFE for five minutes resulted in some unique attributes including excellent piezoelectric performance, uniformity in the nanocomposites and high production efficiency. The composites were formed by mixing rGO dropwise into the PVDF-TrFE solutions, followed by forming homogeneous solutions using the ultrasonication process. After the nanocomposites were formed using an optimized amount of rGO, the thin films were coated on the substrates to form a thickness of around 10 microns. Then, in situ polarization process was carried out over these coated films, subsequently followed by peeling off and forming the electrodes using copper wires and silver paste. The surface area of the prototypes was approximately 40 mm x 50 mm. While the crystallinity of these PVDF-TrFE-formed devices was improved, their performances also improved in terms of V_{oc} and power density as compared to pure PVDF-TrFE-based devices. The output voltage increased around 1.6 times, while the power density became twice that of the pure ones.

The popularization of PVDF and rGO composite for forming PENG can also be shown in the development of thin-film device by Kumar et al. [87]. Homogeneity between the 2D nanofillers and polymer chain in the nanocomposites was maintained in order to induce the electroactive phases in the polar polymer. Some of the advantages of the sensors were low standing stability and high linearity in the responses. After the preparation of the nanofillers and nanohybrids, the devices were formed. PVDF and nanohybrids were molded into thin films having a thickness of 100 microns. The nanocomposites were then cut into specific dimensions, and a silver layer was attached on both sides of the thin films. The FTIR spectrum confirmed electroactive phase with the peaks obtained at 840 cm^{-1} and 884 cm^{-1} for the β/γ phase and γ-peak, respectively, for the composites case against 796, 876 and 975 cm^{-1} adsorption peaks for α-phase in pure PVDF. A motor-driven mechanical setup was assembled to determine the voltage and current. The load exerted on the samples was 500 gm in order to obtain a maximum output voltage and current of ±0.45 V and 150 nA, respectively. The devices achieved a high power density of 14 W/cm^3 showcasing their capability of operating as self-power devices.

Along with PVDF, other polymers like polyaniline (PANI) have also been utilized to form highly efficient PENG. One of the recent works [88] showed the formation of PENG using nanocomposites developed by mixing PVDF nanofibers, rGO and PANI. Electrospinning technique was used to mix rGO with the polymers, followed by forming two different types of nanofiber mats. The electrospinning process was carried out with a feeding rate, needle-collector distance, voltage and collector spin rate of 4 ml/hr, 20 cm, 30 kV and 300 rpm, respectively. The first mat was formed by mixing rGO and rGO/PANI-doped PVDF nanofibers and the second mat was formed by mixing rGO, PANI and rGO/PANI-spray-coated PVDF nanofibers. While the differences lied in the synthesis processes, the maximum output voltages obtained by the first and second types of mats were 7.84 V and 10.60 V, respectively. The electrospinning process also assisted in the formation of a β-crystalline phase of PVDF. The first type of nanofiber mats had the advantage of higher device accuracy, while the second type of mat had advantages of fast and large-scale industrial production.

Pariy et al. [89] showed the development of PENG devices with hybrid micropillar arrays using PVDF and rGO. rGO used as nucleating fillers helped to develop prototypes having a temperature-induced downward dipole orientation to determine the piezoelectric response of the micropillars. Fig. 7 shows the fabrication steps of the PVDF-based micropillar arrays [89]. The stamp was formed using PDMS replicated from a silicon master featuring pillars. The diameter, height and period of the pillars were 5 microns, 4 microns and 20 microns, respectively. The development of the PVDF micropatterns was done using the dip-coating technique on aluminum foils, followed by heating and applied pressure of 200 kPa to 310 kPa. The amount of rGO was varied between 0.1 wt.% and 0.4 wt.% to study the degree of change of the polarization direction. An optimized value of 0.1 wt.% of rGO was mixed with the polymer matrix to form the composites. While the phase angle was changed from -120˚ to 20˚- 40˚, the pure PVDF and rGO/PDVF-based nanocomposites had a response of 86 pm/V and 87 pm/V respectively, after the low-temperature quenching process.

Another recent work showing the loading of rGO onto PVDF to form nanocomposite films-based PENG can be shown in [90]. rGO was synthesized using sonication assisted method, which later was mixed with PVDF and N, N-dimethylformamide (DMF) under the influence of magnetic

stirring. Solution casting method was opted to develop the devices that had enhancement of β-phase from 53% to 70% due to the addition of rGO nanosheets in the PVDF matrix. This was done by pouring the solution over clean glass substrates and heated in the oven for five hours. The composite films were then cooled and peeled off from the glass substrates and used for characterization and experimental purposes. The average peal voltages were 0.913 V, 1.556 V and 2.180 V for pure PVDF and two composite-based thin-films with different rGO weight percentages. The nanocomposite-based prototypes also showed ferromagnetic behavior due to the increase in the remnant polarization values as compared to the pure PVDF films. The exposure of these devices to ultraviolet light had a maximum output voltage around 13.8% higher than that of the pure PVDF films under the application of the same pressure. Table 1 shows a summary of the performances of the rGO composite-based PENG energy-harvesting devices.

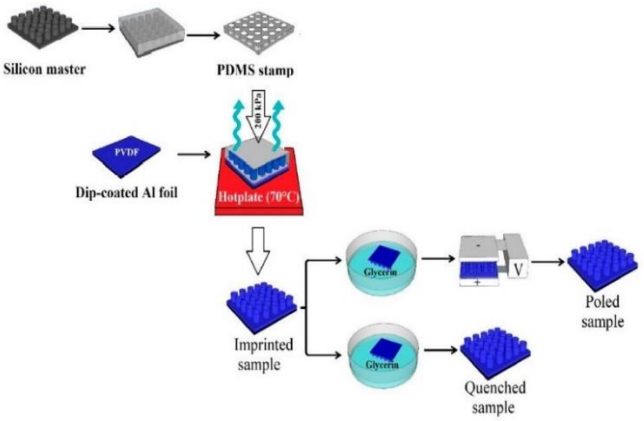

Fig. 7. Schematic diagram of the fabrication process of the PVDF micropillar arrays [89].

TABLE 1
SUMMARY OF THE PERFORMANCES OF THE RGO COMPOSITE-BASED DEVICES OPERATING UNDER THE PIEZOELECTRIC PRINCIPLE

Ref.	Materials	Peak Volt. (V)	Peak Curr. (μA)	Max Pow. Dens. (W/m^3)	Performance compared to the case without rGO
[24]	rGO, Ag NP, PVDF, PDMS, Al	18	1.05	28	NA
[25]	rGO, PVDF-TrFE, ITO, PET	89.7	0.92	340	22× voltage
[75]	rGO, PVDF-TrFE, ITO	8.3	0.6	28.7	1.6× voltage; 2× power
[86]	rGO, PVDF-TrFE, $BaTiO_3$, PDMS, Au, Cu	8.5	2	NA	NA
[87]	rGO, PVDF	0.45	0.15	14	NA

B. Examples of TENG energy-harvesters

The work shown by Hwang et al. [91] highlighted the use of highly porous rGO films for developing shape-adaptive TENG. Fig. 8 depicts the synthesis process of the TENG based on rGO thin-films [91]. A solvent casting method was used to form the devices that had foldable features up to $1/16^{th}$ of their size. The thickness of these rGO films was optimized between 5 microns and 30 microns to correspondingly improve the electrical properties. The devices had a surface area of 13 cm x 3 cm. Other advantages such as low work function, high carrier concentration and high surface area of the prototypes led to the generation of a high output voltage, current, and power of 81.5 V, 3.9 μA/cm^2, and 255 μW/cm^2, respectively. The annealing of these devices led to a further decrease of the work function and an increase in the charge concentration. The films were highly durable in nature, having stable responses in terms of output voltage and electrical conductivity even after 100000 cycles. The prototypes were attached inside the arm of a person to analyze their shape-adaptive characteristics. They were able to generate an output voltage of 170 V, which was enough to turn 19 green LEDs.

Fig. 8. Representation of the fabrication process of the solvent casting/rGO films- based TENG [91].

Another interesting work on the deployment of rGO-based TENG could be seen in [79]. Some of the advantages of these devices included the simple assembly, high mechanical flexibility and high structural stability. GO synthesized using the modified Hummers' method was purified and calcined to form rGO sheets. The rGO films consisted of exfoliated and dispersive graphene sheets on nickel foam substrates. Two individual effects, including the strain effect of graphene sheets and the triboelectric effect between the graphene and electrolyte, were used for energy harvesting purpose. The working, counter and reference electrodes were formed using rGO/nickel foam, platinum plate and Ag/AgCl electrodes, respectively. During the experimental process, an external force was exerted in order to maintain the electrolyte under the stirring process. This produced a frictional force between the rGO sheets and the electrolyte, which generated an electrical output.

Other than the polymeric interference, nanoparticles have also helped to develop high-quality rGO-based TENG for energy-harvesting applications. Keshvari et al. [92] showed the use of rGO/Ag NPs composite for the fabrication of a plasmonic self-powered UV detector. A highly sensitive photoconductive layer was formed using the nanocomposite heterostructures via plasmon-assisted photo-response. After the Ag NPs and rGO were synthesized using the solution and modified Hummers' methods, respectively, PDMS was formed and spin-coated on ITO-coated glass and cured at 100 ˚C for 35 min. Two crucial steps of drop-casting and dip-coating were then performed with the Ag NPs and rGO, respectively, to form the resultant composites. The two surfaces coming in contact with each other consisted of steel and rGO electrodes. The inclusion of the Ag NPs with rGO improved the output voltage of the TENG by a factor of 5. It was also discovered that combining rGO and Ag NPs increased photo responsiveness,

which was attributed to the activation of localized surface plasmons in Ag NPs, which might result in plasmon-assisted photodesorption of remaining oxygen groups from the surface of rGO sheets. A 50% improvement in sensitivity was reported under UV light illumination with a power density of 500 $\mu W/cm^2$.

Apart from PDMS, polyimide (PI) was also used to develop efficient TENG, as shown by Wu et al. [93]. The rGO was used as a frictional layer to trap the electrodes generated on the surface of the PI layer. Fig. 9 shows the schematic illustration of the different layers of the fabricated TENG [93]. While GO was prepared using the modified Hummers' method, PI was formed from polyamide acid (PAA) as a precursor material. PAA was reacted with other compounds like DMF, p-phenylenediamine and biphynultetracarboxylic dianhydride, followed by mixing them with GO mixture and GO sheets. The deposition of GO film was done on PI film using the spin-coating method, followed by baking them at 135 ˚C for 30 min. The active size of the lateral-sliding mode TENG was around 1.5 cm x 2.5 cm. The bottom layer was formed with glass substrates, whereas electrodes formed using aluminium and PI/rGO-stacked structure. The characterization of the prototypes was done at frequencies less than 7 Hz. The device had a maximum output power density of 6.3 W/m^2, which was around 30 times higher than the prototypes formed with rGO sheets. A maximum V_{oc} of 190 V was achieved with this prototype, which was around seven times higher than that of the ones formed with rGO sheets.

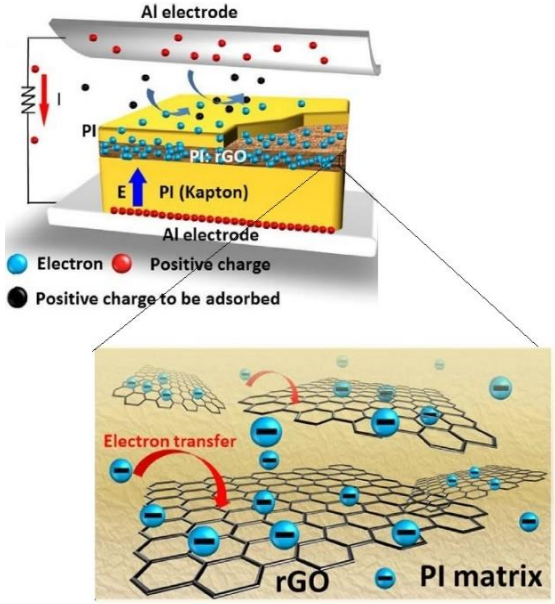

Fig. 9. Illustration of the vertical contact-separation mode TENG formed with a layer of rGO sheets [93].

The optimization of the harvested energy was done using prototypes developed from a composite comprising wrinkled PDMS and rGO [94]. The nanocomposites possessed certain properties like optimized hydrophobicity and ameliorated dielectric properties as a result of optimized values of rGO in the PDMS matrix. This optimization process was achieved by determining certain parameters like thicknesses of rGO, polymer, nanocomposite samples, water contact angles, dielectric properties and triboelectric responses. Fig. 10 shows the schematic diagram of the fabrication process of the rGO/PDMS-based TENG device [94]. The sample had silicon substrates on which the nanocomposites were drop-casted. The devices were then heated and attached to gold electrodes from one side and with platinum wires and silver glue on the other side. The total surface area of these devices was 2 cm x 2 cm. The optimal value of rGO incorporated in the PDMS matrix was 0.5 mg, whereas the thickness of PDMS was around 141 microns with a higher water contact angle of 116.9˚. The electrical conductivity of the triboelectric film was 0.32 S/m. The highest V_{oc} and I_{sc} obtained with these devices were 2 V and 2 nA, respectively, for the rolling water being in contact and separation with the surface of the nanocomposites. Table 2 shows a summary of the performances of the rGO composite-based TENG energy-harvesting devices.

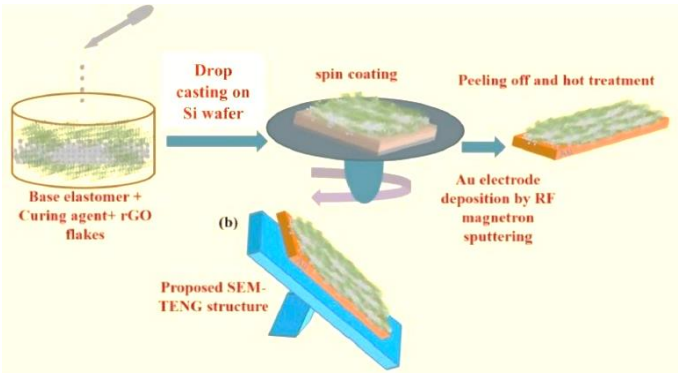

Fig. 10. Representation of the synthesis process of the PDMS/rGO-based TENG for optimization of harvesting energy [94].

TABLE 2
SUMMARY OF THE PERFORMANCES OF THE RGO COMPOSITE-BASED DEVICES OPERATING UNDER THE TRIBOELECTRIC PRINCIPLE

Ref.	Materials	Peak Volt. (V)	Peak Curr. (μA)	Max. Pow. Dens. (W/m^2)	Performance compared to the case without rGO
[79]	rGO, PTFE, Ni	0.040	28	NA	NA
[91]	rGO, PTFE, Al	81.5	3.9/cm^2	2.55	1.4× power
[92]	rGO, steel, PDMS, ITO, Glass, Ag NP	10	NA	NA	NA
[93]	rGO, Al, Pl	90	NA	6.3	30× power
[94]	rGO, PDMS, Au	1	0.002	NA	1.25× voltage

V. CHALLENGES AND FUTURE OPPORTUNITIES

Although a substantial amount of work has been done regarding the use of rGO-based composites for energy-harvesting applications, there are still certain loopholes that need to be addressed in the current scenario. Firstly, the electromechanical characteristics of rGO are inferior as compared to that of pure graphene, so the efficiency of the prototypes would be increased with the inclusion of pure graphene in the composites. Some of the limitations of nanogenerators as operating devices are their low term unreliability and low durability. These prototypes happen to be fragile and have operated mostly in controlled environments. Prototypes have to be developed, which can be deployed as

wearable sensors in real-time conditions to harvest energy from physiological body movements. The consideration of polymers for forming PENG and TENG should also be done tactfully so as to avoid the reduction in electrical conductivity of the resultant nanocomposites. The percolation threshold of each of the rGO in the polymer matrix should be further analyzed with different polymers for as other local and intrinsic factors should also be taken into account during the study. In terms of application, the energy-harvesting sensors should be integrated more with biomedical sensing systems as they would assist in the operation of these biosensors for a longer period. Certain flexible biosensors like catheters, which are inserted inside the human body, can be operated ubiquitously if these energy-harvesters are attached to the them for continuous power. The vibrational motions of these devices inside the body would help the PENG and TENG-based devices to induce voltage for operational purposes. These devices should be further used as wearable sensors that can be used as compact-sized power suppliers for prototypes operating in conditions where it is difficult to install wires.

The global market survey of energy harvesters shows that there is high rise in the use of these devices in different industrial verticals such as mechanical engineering, consumer electronics, textile and biomedical industries [95, 96]. The rising issues like global warming and energy crises makes it a state-of-the-art to opt for renewable resources that can not only assist in the reduction of carbon emission, but also provide an alternative source of energy over a wide range of scales. With the integration of these sensors with other disciplines like internet of things (IoT), they can bring about a revolutionary change in the quality of human life.

VI. Conclusion

The paper presents the work done on the design, development and implementation of mechanical energy harvesters made from rGO material, particularly those based on piezoelectric and triboelectric mechanisms. The properties of rGO that render it viable candidate for the development of highly efficient energy harvesting devices have been elucidated. Some notable examples have been displayed to demonstrate the breadth of processed materials and fabrication techniques used to construc the prototypes. The advancements made thus far in this area have paved the way for self-powered wearable electronics.

References

[1] J. A. Paradiso and T. Starner, "Energy scavenging for mobile and wireless electronics," *IEEE Pervasive Computing*, vol. 4, no. 1, pp. 18-27, 2005.

[2] C. Ó. Mathúna, T. O'Donnell, R. V. Martinez-Catala, J. Rohan, and B. O'Flynn, "Energy scavenging for long-term deployable wireless sensor networks," *Talanta*, vol. 75, no. 3, pp. 613-623, 2008.

[3] T. Ghomian and S. Mehraeen, "Survey of energy scavenging for wearable and implantable devices," *Energy*, vol. 178, pp. 33-49, 2019.

[4] D. Jia and J. Liu, "Human power-based energy harvesting strategies for mobile electronic devices," *Frontiers of Energy and Power Engineering in China*, vol. 3, no. 1, pp. 27-46, 2009.

[5] R. J. M. Vullers, R. van Schaijk, I. Doms, C. Van Hoof, and R. Mertens, "Micropower energy harvesting," *Solid-State Electronics*, vol. 53, no. 7, pp. 684-693, 2009.

[6] K. V. Selvan and M. S. Mohamed Ali, "Micro-scale energy harvesting devices: Review of methodological performances in the last decade," *Renewable and Sustainable Energy Reviews*, vol. 54, pp. 1035-1047, 2016.

[7] S. Chandrasekaran *et al.*, "Micro-scale to nano-scale generators for energy harvesting: Self powered piezoelectric, triboelectric and hybrid devices," *Physics Reports*, vol. 792, pp. 1-33, 2019.

[8] A. M. Zamarayeva *et al.*, "Flexible and stretchable power sources for wearable electronics," *Science Advances*, vol. 3, no. 6, p. e1602051, 2017.

[9] J. Li, J. Zhao, and J. A. Rogers, "Materials and Designs for Power Supply Systems in Skin-Interfaced Electronics," *Accounts of Chemical Research*, vol. 52, no. 1, pp. 53-62, 2019.

[10] Z. Li, Q. Zheng, Z. L. Wang, and Z. Li, "Nanogenerator-Based Self-Powered Sensors for Wearable and Implantable Electronics," *Research*, vol. 2020, p. 8710686, 2020.

[11] Y. Song *et al.*, "Wireless battery-free wearable sweat sensor powered by human motion," *Science advances*, vol. 6, no. 40, p. eaay9842, 2020.

[12] Z. Lin *et al.*, "Broadband and three-dimensional vibration energy harvesting by a non-linear magnetoelectric generator," *Applied Physics Letters*, vol. 109, no. 25, p. 253903, 2016.

[13] L. C. Rome, L. Flynn, E. M. Goldman, and T. D. Yoo, "Generating Electricity While Walking with Loads," *Science*, vol. 309, no. 5741, p. 1725, 2005.

[14] S. Meninger, J. O. Mur-Miranda, R. Amirtharajah, A. Chandrakasan, and J. H. Lang, "Vibration-to-electric energy conversion," *IEEE Transactions on Very Large Scale Integration (VLSI) Systems*, vol. 9, no. 1, pp. 64-76, 2001.

[15] L. G. W. Tvedt, D. S. Nguyen, and E. Halvorsen, "Nonlinear Behavior of an Electrostatic Energy Harvester Under Wide- and Narrowband Excitation," *Journal of Microelectromechanical Systems*, vol. 19, no. 2, pp. 305-316, 2010.

[16] A. T. Le, M. Ahmadipour, and S.-Y. Pung, "A review on ZnO-based piezoelectric nanogenerators: Synthesis, characterization techniques, performance enhancement and applications," *Journal of Alloys and Compounds*, p. 156172, 2020.

[17] Y. Song, Z. Shi, G.-H. Hu, C. Xiong, A. Isogai, and Q. Yang, "Recent advances in cellulose-based piezoelectric and triboelectric nanogenerators for energy harvesting: a review," *Journal of Materials Chemistry A*, 2021.

[18] A. A. Mathew, A. Chandrasekhar, and S. Vivekanandan, "A Review on Real-Time Implantable and Wearable Health Monitoring Sensors based on Triboelectric Nanogenerator Approach," *Nano Energy*, p. 105566, 2020.

[19] S. Rathore, S. Sharma, B. P. Swain, and R. K. Ghadai, "A critical review on triboelectric nanogenerator," in *IOP Conf. Ser. Mater. Sci. Eng*, 2018, vol. 377, p. 012186.

[20] Z. L. Wang, "Triboelectric Nanogenerators as New Energy Technology for Self-Powered Systems and as Active Mechanical and Chemical Sensors," *ACS Nano*, vol. 7, no. 11, pp. 9533-9557, 2013.

[21] K. A. Cook-Chennault, N. Thambi, and A. M. Sastry, "Powering MEMS portable devices—a review of non-regenerative and regenerative power supply systems with special emphasis on piezoelectric energy harvesting systems," *Smart Materials and Structures*, vol. 17, no. 4, p. 043001, 2008.

[22] S. R. Anton and H. A. Sodano, "A review of power harvesting using piezoelectric materials (2003–2006)," *Smart Materials and Structures*, vol. 16, no. 3, pp. R1-R21, 2007.

[23] Z. L. Wang and J. Song, "Piezoelectric Nanogenerators Based on Zinc Oxide Nanowire Arrays," *Science*, vol. 312, no. 5771, p. 242, 2006.

[24] M. Pusty, L. Sinha, and P. M. Shirage, "A flexible self-poled piezoelectric nanogenerator based on a rGO–Ag/PVDF nanocomposite," *New Journal of Chemistry*, vol. 43, no. 1, pp. 284-294, 2019.

[25] R. Bhunia, S. Gupta, B. Fatma, Prateek, R. K. Gupta, and A. Garg, "Milli-watt power harvesting from dual triboelectric and piezoelectric effects of multifunctional green and robust reduced graphene oxide/P (VDF-TrFE) composite flexible films," *ACS applied materials & interfaces*, vol. 11, no. 41, pp. 38177-38189, 2019.

[26] D. Zhang, Z. Xu, Z. Yang, and X. Song, "High-performance flexible self-powered tin disulfide nanoflowers/reduced graphene oxide nanohybrid-based humidity sensor driven by triboelectric nanogenerator," *Nano Energy*, vol. 67, p. 104251, 2020.

[27] Y. Gao and Z. L. Wang, "Electrostatic Potential in a Bent Piezoelectric Nanowire. The Fundamental Theory of Nanogenerator and Nanopiezotronics," *Nano Letters*, vol. 7, no. 8, pp. 2499-2505, 2007.

[28] X. Chen, S. Xu, N. Yao, and Y. Shi, "1.6 V Nanogenerator for Mechanical Energy Harvesting Using PZT Nanofibers," *Nano Letters*, vol. 10, no. 6, pp. 2133-2137, 2010.

[29] Y. He *et al.*, "Porous carbon nanosheets: Synthetic strategies and electrochemical energy related applications," *Nano Today*, vol. 24, pp. 103-119, 2019.

[30] X. Wang, J. Song, F. Zhang, C. He, Z. Hu, and Z. Wang, "Electricity Generation based on One-Dimensional Group-III Nitride Nanomaterials," *Advanced Materials*, vol. 22, no. 19, pp. 2155-2158, 2010.

[31] C.-T. Huang *et al.*, "GaN Nanowire Arrays for High-Output Nanogenerators," *Journal of the American Chemical Society*, vol. 132, no. 13, pp. 4766-4771, 2010.

[32] Y.-F. Lin, J. Song, Y. Ding, S.-Y. Lu, and Z. L. Wang, "Alternating the Output of a CdS Nanowire Nanogenerator by a White-Light-Stimulated Optoelectronic Effect," *Advanced Materials*, vol. 20, no. 16, pp. 3127-3130, 2008.

[33] R. Zhang and H. Olin, "Material choices for triboelectric nanogenerators: A critical review," *EcoMat*, vol. 2, no. 4, p. e12062, 2020.

[34] K. S. Novoselov *et al.*, "Electric Field Effect in Atomically Thin Carbon Films," *Science*, vol. 306, no. 5696, p. 666, 2004.

[35] X. Ji, Y. Xu, W. Zhang, L. Cui, and J. Liu, "Review of functionalization, structure and properties of graphene/polymer composite fibers," *Composites Part A: Applied Science and Manufacturing*, vol. 87, pp. 29-45, 2016.

[36] Y. Zhu *et al.*, "Graphene and Graphene Oxide: Synthesis, Properties, and Applications," *Advanced Materials*, vol. 22, no. 35, pp. 3906-3924, 2010.

[37] T. Kuilla, S. Bhadra, D. Yao, N. H. Kim, S. Bose, and J. H. Lee, "Recent advances in graphene based polymer composites," *Progress in Polymer Science*, vol. 35, no. 11, pp. 1350-1375, 2010.

[38] R. J. Young, I. A. Kinloch, L. Gong, and K. S. Novoselov, "The mechanics of graphene nanocomposites: a review," *Composites Science and Technology*, vol. 72, no. 12, pp. 1459-1476, 2012.

[39] B. M. Yoo, H. J. Shin, H. W. Yoon, and H. B. Park, "Graphene and graphene oxide and their uses in barrier polymers," *Journal of Applied Polymer Science*, vol. 131, no. 1, 2014.

[40] A. Nag, A. Mitra, and S. C. Mukhopadhyay, "Graphene and its sensor-based applications: A review," *Sensors and Actuators A: Physical*, vol. 270, pp. 177-194, 2018.

[41] S. K. Krishnan, E. Singh, P. Singh, M. Meyyappan, and H. S. Nalwa, "A review on graphene-based nanocomposites for electrochemical and fluorescent biosensors," *RSC advances*, vol. 9, no. 16, pp. 8778-8881, 2019.

[42] M. M. Islam, S. S. Ahmed, M. Rashid, and M. M. Akanda, "Mechanical and Thermal Properties of Graphene over Composite Materials: A Technical Review," *Journal of Casting & Materials Engineering*, vol. 3, no. 1, p. 19, 2019.

[43] A. T. Lawal, "Graphene-based nano composites and their applications. A review," *Biosensors and Bioelectronics*, vol. 141, p. 111384, 2019.

[44] A. T. Dideikin and A. Y. Vul', "Graphene Oxide and Derivatives: The Place in Graphene Family," (in English), *Frontiers in Physics*, Review vol. 6, no. 149, 2019.

[45] M. Tahriri *et al.*, "Graphene and its derivatives: Opportunities and challenges in dentistry," *Materials Science and Engineering: C*, vol. 102, pp. 171-185, 2019.

[46] A. Nag, M. E. E. Alahi, and S. C. Mukhopadhyay, "Recent progress in the fabrication of graphene fibers and their composites for applications of monitoring human activities," *Applied Materials Today*, vol. 22, p. 100953, 2021.

[47] H. Huang *et al.*, "Graphene-Based Sensors for Human Health Monitoring," (in English), *Frontiers in Chemistry*, Review vol. 7, no. 399, 2019.

[48] S. P. Beeby, M. J. Tudor, and N. M. White, "Energy harvesting vibration sources for microsystems applications," *Measurement Science and Technology*, vol. 17, no. 12, pp. R175-R195, 2006.

[49] P. Dhiman *et al.*, "Harvesting Energy from Water Flow over Graphene," *Nano Letters*, vol. 11, no. 8, pp. 3123-3127, 2011.

[50] H. Liu, J. Zhong, C. Lee, S.-W. Lee, and L. Lin, "A comprehensive review on piezoelectric energy harvesting technology: Materials, mechanisms, and applications," *Applied Physics Reviews*, vol. 5, no. 4, p. 041306, 2018.

[51] V. Vivekananthan, A. Chandrasekhar, N. R. Alluri, Y. Purusothaman, G. Khandelwal, and S.-J. Kim, "Triboelectric Nanogenerators: Design, Fabrication, Energy Harvesting, and Portable-Wearable Applications," in *Nanogenerators*: IntechOpen, 2020.

[52] D. Jiang, B. Shi, H. Ouyang, Y. Fan, Z. L. Wang, and Z. Li, "Emerging Implantable Energy Harvesters and Self-Powered Implantable Medical Electronics," *ACS Nano*, vol. 14, no. 6, pp. 6436-6448, 2020.

[53] X.-Q. Fang, J.-X. Liu, and V. Gupta, "Fundamental formulations and recent achievements in piezoelectric nano-structures: a review," *Nanoscale*, vol. 5, no. 5, pp. 1716-1726, 2013.

[54] J. Briscoe and S. Dunn, "Piezoelectric nanogenerators–a review of nanostructured piezoelectric energy harvesters," *Nano Energy*, vol. 14, pp. 15-29, 2015.

[55] R. Amirtharajah, J. Wenck, J. Collier, J. Siebert, and B. Zhou, "Circuits for energy harvesting sensor signal processing," in *2006 43rd ACM/IEEE Design Automation Conference*, 2006, pp. 639-644.

[56] S. Niyogi, E. Bekyarova, M. E. Itkis, J. L. McWilliams, M. A. Hamon, and R. C. Haddon, "Solution Properties of Graphite and Graphene," *Journal of the American Chemical Society*, vol. 128, no. 24, pp. 7720-7721, 2006.

[57] R. Ruoff, "Calling all chemists," *Nature Nanotechnology*, vol. 3, no. 1, pp. 10-11, 2008.

[58] A. Lerf, H. He, M. Forster, and J. Klinowski, "Structure of Graphite Oxide Revisited," *The Journal of Physical Chemistry B*, vol. 102, no. 23, pp. 4477-4482, 1998.

[59] D. R. Dreyer, S. Park, C. W. Bielawski, and R. S. Ruoff, "The chemistry of graphene oxide," *Chemical Society Reviews*, vol. 39, no. 1, pp. 228-240, 2010.

[60] S. Stankovich, R. D. Piner, X. Chen, N. Wu, S. T. Nguyen, and R. S. Ruoff, "Stable aqueous dispersions of graphitic nanoplatelets via the reduction of exfoliated graphite oxide in the presence of poly(sodium 4-styrenesulfonate)," *Journal of Materials Chemistry*, vol. 16, no. 2, pp. 155-158, 2006.

[61] S. Park and R. S. Ruoff, "Chemical methods for the production of graphenes," *Nature Nanotechnology*, vol. 4, no. 4, pp. 217-224, 2009.

[62] S. Gilje, S. Han, M. Wang, K. L. Wang, and R. B. Kaner, "A Chemical Route to Graphene for Device Applications," *Nano Letters*, vol. 7, no. 11, pp. 3394-3398, 2007.

[63] H. A. Becerril, J. Mao, Z. Liu, R. M. Stoltenberg, Z. Bao, and Y. Chen, "Evaluation of Solution-Processed Reduced Graphene Oxide Films as Transparent Conductors," *ACS Nano*, vol. 2, no. 3, pp. 463-470, 2008.

[64] J. Zhao, S. Pei, W. Ren, L. Gao, and H.-M. Cheng, "Efficient Preparation of Large-Area Graphene Oxide Sheets for Transparent Conductive Films," *ACS Nano*, vol. 4, no. 9, pp. 5245-5252, 2010.

[65] J. T. Robinson, F. K. Perkins, E. S. Snow, Z. Wei, and P. E. Sheehan, "Reduced Graphene Oxide Molecular Sensors," *Nano Letters*, vol. 8, no. 10, pp. 3137-3140, 2008.

[66] J. R. Lomeda, C. D. Doyle, D. V. Kosynkin, W.-F. Hwang, and J. M. Tour, "Diazonium Functionalization of Surfactant-Wrapped Chemically Converted Graphene Sheets," *Journal of the American Chemical Society*, vol. 130, no. 48, pp. 16201-16206, 2008.

[67] S. Stankovich *et al.*, "Graphene-based composite materials," *Nature*, vol. 442, no. 7100, pp. 282-286, 2006.

[68] G. Wang *et al.*, "Facile Synthesis and Characterization of Graphene Nanosheets," *The Journal of Physical Chemistry C*, vol. 112, no. 22, pp. 8192-8195, 2008.

[69] R. Muszynski, B. Seger, and P. V. Kamat, "Decorating Graphene Sheets with Gold Nanoparticles," *The Journal of Physical Chemistry C*, vol. 112, no. 14, pp. 5263-5266, 2008.

[70] H. C. Schniepp *et al.*, "Functionalized Single Graphene Sheets Derived from Splitting Graphite Oxide," *The Journal of Physical Chemistry B*, vol. 110, no. 17, pp. 8535-8539, 2006.

[71] M. J. McAllister *et al.*, "Single Sheet Functionalized Graphene by Oxidation and Thermal Expansion of Graphite," *Chemistry of Materials*, vol. 19, no. 18, pp. 4396-4404, 2007.

[72] G. Williams, B. Seger, and P. V. Kamat, "TiO2-Graphene Nanocomposites. UV-Assisted Photocatalytic Reduction of Graphene Oxide," *ACS Nano*, vol. 2, no. 7, pp. 1487-1491, 2008.

[73] L. Fu *et al.*, "Realization of Ambient-Stable Room-Temperature Ferromagnetism by Low-Temperature Annealing of Graphene Oxide Nanoribbons," *ACS Nano*, vol. 13, no. 6, pp. 6341-6347, 2019.

[74] G. Eda, G. Fanchini, and M. Chhowalla, "Large-area ultrathin films of reduced graphene oxide as a transparent and flexible electronic material," *Nature Nanotechnology*, vol. 3, no. 5, pp. 270-274, 2008.

[75] X. Hu, Z. Ding, L. Fei, and Y. Xiang, "Wearable piezoelectric nanogenerators based on reduced graphene oxide and in situ polarization-enhanced PVDF-TrFE films," *Journal of materials science*, vol. 54, no. 8, pp. 6401-6409, 2019.

[76] N. An, H. Liu, Y. Ding, M. Zhang, and Y. Tang, "Preparation and electroactive properties of a PVDF/nano-TiO2 composite film," *Applied Surface Science*, vol. 257, no. 9, pp. 3831-3835, 2011.

[77] A. P. Indolia and M. S. Gaur, "Investigation of structural and thermal characteristics of PVDF/ZnO nanocomposites," *Journal of Thermal Analysis and Calorimetry*, vol. 113, no. 2, pp. 821-830, 2013.

[78] S. K. Karan *et al.*, "An Approach to Design Highly Durable Piezoelectric Nanogenerator Based on Self-Poled PVDF/AlO-rGO Flexible Nanocomposite with High Power Density and Energy Conversion Efficiency," *Advanced Energy Materials*, vol. 6, no. 20, p. 1601016, 2016.

[79] W. Li, Y. Zhang, L. Liu, D. Li, L. Liao, and C. Pan, "A high energy output nanogenerator based on reduced graphene oxide," *Nanoscale*, vol. 7, no. 43, pp. 18147-18151, 2015.

[80] C. Wu, F. Li, T. Guo, and T. W. Kim, "Controlling memory effects of three-layer structured hybrid bistable devices based on graphene sheets sandwiched between two laminated polymer layers," *Organic Electronics*, vol. 13, no. 1, pp. 178-183, 2012.

[81] H. Jiang *et al.*, "Charge-trapping-blocking layer for enhanced triboelectric nanogenerators," *Nano Energy*, vol. 75, p. 105011, 2020.
[82] M. El-hami *et al.*, "Design and fabrication of a new vibration-based electromechanical power generator," *Sensors and Actuators A: Physical*, vol. 92, no. 1, pp. 335-342, 2001.
[83] S. Roundy, P. K. Wright, and K. S. J. Pister, "Micro-Electrostatic Vibration-to-Electricity Converters," in *ASME 2002 International Mechanical Engineering Congress and Exposition*, 2002, vol. Microelectromechanical Systems, pp. 487-496.
[84] J. Luo and Z. L. Wang, "Recent progress of triboelectric nanogenerators: From fundamental theory to practical applications," *EcoMat*, vol. 2, no. 4, p. e12059, 2020.
[85] Y. Zi and Z. L. Wang, "Nanogenerators: An emerging technology towards nanoenergy," *Apl Materials*, vol. 5, no. 7, p. 074103, 2017.
[86] U. Yaqoob and G.-S. Chung, "Effect of reduced graphene oxide on the energy harvesting performance of P (VDF-TrFE)-BaTiO3 nanocomposite devices," *Smart Materials and Structures*, vol. 26, no. 9, p. 095060, 2017.
[87] C. Kumar, A. Gaur, S. K. Rai, and P. Maiti, "Piezo devices using poly (vinylidene fluoride)/reduced graphene oxide hybrid for energy harvesting," *Nano-Structures & Nano-Objects*, vol. 12, pp. 174-181, 2017.
[88] Ö. F. Ünsal, Y. Altın, and A. Çelik Bedeloğlu, "Poly (vinylidene fluoride) nanofiber-based piezoelectric nanogenerators using reduced graphene oxide/polyaniline," *Journal of Applied Polymer Science*, vol. 137, no. 13, p. 48517, 2020.
[89] I. O. Pariy *et al.*, "Piezoelectric response in hybrid micropillar arrays of poly (vinylidene fluoride) and reduced graphene oxide," *Polymers*, vol. 11, no. 6, p. 1065, 2019.
[90] A. Anand, D. Meena, K. K. Dey, and M. C. Bhatnagar, "Enhanced piezoelectricity properties of reduced graphene oxide (RGO) loaded polyvinylidene fluoride (PVDF) nanocomposite films for nanogenerator application," *Journal of Polymer Research*, vol. 27, no. 12, pp. 1-11, 2020.
[91] H. J. Hwang, J. S. Yeon, Y. Jung, H. S. Park, and D. Choi, "Extremely Foldable and Highly Porous Reduced Graphene Oxide Films for Shape-Adaptive Triboelectric Nanogenerators," *Small*, p. 1903089, 2020.
[92] A. Keshvari, S. Darbari, and M. Taghavi, "Self-powered plasmonic UV detector, based on reduced graphene oxide/Ag nanoparticles," *IEEE Electron Device Letters*, vol. 39, no. 9, pp. 1433-1436, 2018.
[93] C. Wu, T. W. Kim, and H. Y. Choi, "Reduced graphene-oxide acting as electron-trapping sites in the friction layer for giant triboelectric enhancement," *Nano Energy*, vol. 32, pp. 542-550, 2017.
[94] A. N. Parvez, M. H. Rahaman, H. C. Kim, and K. K. Ahn, "Optimization of triboelectric energy harvesting from falling water droplet onto wrinkled polydimethylsiloxane-reduced graphene oxide nanocomposite surface," *Composites Part B: Engineering*, vol. 174, p. 106923, 2019.
[95] Businesswire. "Triboelectric Nanogenerator Market - Forecasts from 2020 to 2025." Available online: https://www.businesswire.com/news/home/20210302005572/en/134.11-Million-Triboelectric-Nanogenerator-Markets-2025---Market-to-Grow-at-a-CAGR-of-48.55---ResearchAndMarkets.com (accessed 10 April 2021).
[96] MarketsandMarkets. "Piezoelectric Devices Market." Available online: https://www.marketsandmarkets.com/Market-Reports/piezoelectric-devices-market-256019882.html (accessed 5 April 2021).